Journal of the Neurological Sciences 398 (2019) 9–15

Contents lists available at ScienceDirect

Journal of the Neurological Sciences

journal homepage: www.elsevier.com/locate/jns

Location-specific characteristics of perivascular spaces as the brain's interstitial fluid drainage system

Shigeki Yamada[a,b,d,*], Masatsune Ishikawa[a,c], Kazuo Yamamoto[b], Makoto Yamaguchi[b], Marie Oshima[d]

[a] Normal Pressure Hydrocephalus Center, Rakuwakai Otowa Hospital, Kyoto, Japan
[b] Department of Neurosurgery and Stroke Center, Rakuwakai Otowa Hospital, Kyoto, Japan
[c] Rakuwakai Healthcare System, Rakuwa Villa Ilios, Kyoto, Japan
[d] Interfaculty Initiative in Information Studies / Institute of Industrial Science, The University of Tokyo, Tokyo, Japan

ARTICLE INFO

Keywords:
Glymphatic pathway
Perivascular space
Leukoaraiosis
Centrum semiovale
White matter hyperintensity
Magnetic resonance imaging

ABSTRACT

Purpose: Brain interstitial fluid plays an important role in the excretion of metabolic waste products into the cerebrospinal fluid through perivascular spaces (PVS). To investigate the normal function of PVS in healthy elderly individuals, we assessed the relationship between PVS and white matter hyperintensity (WMH) on MRI in two locations.

Methods: This study included 296 healthy individuals aged ≥60 years without a history of brain disease who underwent brain MRI. The severities of PVS and WMH were assessed on the location-specific classification in the basal ganglia (BG-PVS) or centrum semiovale (CSO-PVS), and in the deep or periventricular WMH.

Results: The severity of BG-PVS was significantly associated with the severities of deep and periventricular WMHs. In contrast, the severity of CSO-PVS was inversely associated with the severity of deep WMH and was not significantly associated with that of periventricular WMH. The multivariate odds ratios of severe deep WMH for BG-PVS and CSO-PVS were 1.18 (95% CIs: 1.01–1.38) and 0.68 (0.54–0.86), respectively, compared with none deep WMH.

Conclusions: CSO-PVS looks different from BG-PVS in their relationship with deep WMHs. Therefore, CSO-PVS might play an essential role in the normal interstitial fluid drainage system, not as a biomarker of arteriosclerosis.

1. Introduction

Brain fluid dynamics have been elucidated in this century. In particular, studying the glymphatic pathway through the perivascular spaces (PVS) surrounding cerebral arteries and veins contributes to our understanding of the mechanisms of brain interstitial fluid homeostasis [1–3]. Concretely, brain interstitial fluid plays an important role as a water cooling system and a sink for drainage of the neurotoxic compounds such as amyloid-ß or phosphorylated tau in cooperation with cerebrospinal fluid [4]. However, this reciprocal fluid exchange in the subarachnoid and interstitial spaces via the PVS has been primarily observed near the cortical surface and not in the deep subcortical white matter regions [4,5]. Accordingly, the function of PVS in the deep white matter has not been completely elucidated, although dilated PVS are believed to be associated with aging, arteriosclerosis and several vascular risk factors. [6–14] On the other hand, white matter hyperintensity (WMH) on magnetic resonance imaging (MRI) is also reported to be representative of changes associated with aging and small vessel diseases, such as disruption of the blood-brain barrier, perivascular damage, and amyloid angiopathy [8,12,15,16]. The presence and severity of WMH have been reported to be strongly associated with dilated PVS, although both dilated PVS and WMH on MRI might be different in function and mechanism by location, i.e. basal ganglia, periventricular lesion or deep white matter around the centrum

Abbreviations: BG, basal ganglia; CSO, centrum semiovale; DBP, diastolic blood pressure; eGFR, estimated glomerular filtration rate; FLAIR, fluid-attenuated inversion recovery; MRI, magnetic resonance imaging; PVS, perivascular space; SBP, systolic blood pressure; SD, standard deviation; T, tesla; WMH, white matter hyperintensity

* Corresponding author at: Rakuwakai Otowa Hospital, Normal Pressure Hydrocephalus Center and Department of Neurosurgery, Otowachinji-cho 2, Yamashina-ku, Kyoto 607-8062, Japan

E-mail addresses: shigekiyamada39@gmail.com (S. Yamada), rakuwadr1001@rakuwadr.com (M. Ishikawa), y_makoto@kuhp.kyoto-u.ac.jp (M. Yamaguchi), marie@iis.u-tokyo.ac.jp (M. Oshima).

https://doi.org/10.1016/j.jns.2019.01.022
Received 19 September 2018; Received in revised form 11 December 2018; Accepted 14 January 2019
Available online 16 January 2019
0022-510X/

semiovale [8,11,13,15,17–19]. Therefore, we evaluated the location-specific association between PVS and WMH in the healthy elderly individuals to elucidate the mechanisms of interstitial fluid homeostasis in aging brains.

2. Material and methods

2.1. Study population

The study design and protocol were approved by the ethics committee for human research at our institute. The clinical data collection has been described in detail in our prior publication [20]. In brief, 1079 consecutive healthy Japanese underwent a brain MRI examination between March 2015 and February 2017 at our health screening center for the purpose of a brain check-up. The inclusion criteria for this study required participants to be 60 years of age or older and have no past medical history of brain disease, specifically stroke. Among 304 individuals aged ≥60 years, 8 subjects who had a medical history of cerebrovascular disease were excluded from this study. Finally, 296 individuals (age range, 60–83 years; 222 men and 74 women) met our inclusion criteria. The clinical data collected at the time of the MRI included the participant's age, height, weight, systolic blood pressure (SBP), diastolic blood pressure (DBP), smoking habits, and medical history of hypertension, dyslipidemia, diabetes mellitus, stroke, and chronic heart disease, for 222 individuals. The estimated glomerular filtration rate (eGFR) was calculated by considering the patient's age, gender, and serum creatinine level, using the Modification of Diet in Renal Disease Study Group formula: eGFR (mL/min/1.73 m^2) = 186.3 × (serum creatinine [mg/dL]) $^{-1.154}$ × age (years) $^{-0.203}$ × (0.742, if female). The cutoff point used for eGFR was 60 mL/min/1.73 m^2. The cutoff points for SBP and DBP were 130 mmHg and 85 mmHg, respectively. Body mass index (BMI) was calculated as the weight in kilograms divided by height in meters squared (kg/m^2). The cutoff point for BMI was 25.0 kg/m^2.

2.2. MRI data assessment

Of 296 individuals, 124 underwent a brain MRI using a 3-tesla (T) MRI scanner (MAGNETOM Skyra, Siemens AG, Muenchen, Germany), and 172 underwent an MRI using a 1.5T MRI scanner (MAGNETOM Avanto, Siemens AG, Muenchen, Germany). The sequences used for the routine brain check-up were conventional axial images with slice thickness by 5 mm of T1-weighted, T2-weighted, FLAIR, and T2*-weighted gradient-recalled echo sequences. PVS were defined as round, oval, or linear-shaped lesions with a smooth margin and were classified into those around the centrum semiovale (CSO-PVS) or the basal ganglia (BG-PVS). CSO-PVS and BG-PVS were assessed on T2-weighted images after narrowing the window width from 1500 to 250 for 3T MRI and from 1150 to 200 for 1.5T MRI and after changing the window level from 600 to 450 for 3T MRI and from 500 to 300 for 1.5T MRI (Fig. 1A-C). The severity of PVS was classified based on the number of MRI-visible PVS into the following 3 grades: Grade 0: invisible or sparse (PVS ≤ 10), Grade 1: moderate visible (10 < PVS ≤ 30), and Grade 2: abundant visible (PVS > 30), as reported previously [20]. Cohens' kappa coefficients for the inter-rater agreement were 0.81 for CSO-PVS and 0.83 for BG-PVS, respectively. Additionally, PVS were simply assessed using the classification of visible (Grade 1 or 2) or invisible (Grade 0). The severities of WMH were also assessed on a fluid-attenuated inversion recovery (FLAIR) sequence after being classified into periventricular and deep WMH based on their location, according to the Fazekas rating scale, as follows: Grade 0: absent, Grade 1: cap-like periventricular WMH and small focal deep WMH, Grade 2: periventricular WMH encircling lateral ventricles and small confluent deep WMH, Grade 3: irregular periventricular WMH extending into large confluent deep WMH, respectively (Fig. 1D, E) [21]. The presence and number of cerebral microbleeds were evaluated on T2*-weighted gradient-recalled echo sequences after categorization as lobar (cortical-subcortical area) or deep (basal ganglia, thalami, brainstem) (Fig. 1F).

2.3. Statistical analysis

At first, the relationships between PVS and WMH were assessed in each location. The ORs and 95% CIs for the presence and severity of PVS and WMH were calculated by logistic regression analyses. Multivariate analyses were adjusted for age, eGFR, BMI, SBP, DBP, smoking habits, and medical history of hypertension, dyslipidemia, diabetes mellitus, and chronic heart disease, as these are known arteriosclerosis risk factors. In addition, to investigate the effects of sex difference, age-adjusted and multivariate ORs were analyzed after stratification by the sex. Missing data were treated as deficit data that did not affect the prevalence of other variables. Statistical significance was assumed at a probability value (P) of < 0.05 in a Fisher's exact test. All statistical analyses were performed using R software (version 3.3.2; R Foundation for Statistical Computing, Vienna, Austria; http://www.R-project.org).

3. Results

3.1. Clinical characteristics

Among the 296 healthy individuals without stroke, the mean age ± standard deviation (SD) was 66.1 ± 5.9 years old. Other mean clinical values were SBP of 123.0 ± 15.1 mmHg, DBP of 74.3 ± 9.0 mmHg, eGFR of 64.0 ± 22.0 mL/min/1.73 m^2, and BMI of 23.5 ± 3.3 kg/m^2. Table 1 shows the clinical characteristics in each grade of periventricular and deep WMH. Among the participants who had medical histories of hypertension, dyslipidemia and diabetes mellitus, 90%, 89% and 72% underwent medical treatments. The percentage of participants with hypertension tended to be higher for higher grades of deep WMH (31% in Grade 0, 41% in Grade 1 and 55% in Grade 2–3) or periventricular WMH (32% in Grade 0, 46% in Grade 1 and 65% in Grade 2–3). The other clinical variables did not have any significant relationships with the grade of WMH. CSO-PVS was observed in 86% of the all participants, whereas BG-PVS was observed in 70%.

3.2. Relationships between PVS and WMH

Of 108 individuals without deep WMH, 101 (94%) had MRI-visible CSO-PVS and 60 (56%) had MRI-visible BG-PVS. Of 175 individuals without periventricular WMH, 155 (89%) had MRI-visible CSO-PVS and 108 (62%) had MRI-visible BG-PVS. Table 2 shows the relationship between the presence of WMH and the grade of PVS. As the grade of BG-PVS increased, the presence of periventricular and deep WMHs increased gradually. Abundant MRI-visible BG-PVS had the highest multivariate OR (1.60, 95% CI: 1.28–1.99, $P < 0.001$) for the presence of periventricular WMH. In contrast, MRI-visible CSO-PVS had the lowest multivariate OR (0.70, 0.54–0.89 for Grade 1 and 0.87, 0.76–1.00 for Grade 2) for the presence of deep WMH compared with invisible CSO-PVS (i.e., Grade 0). Similarly, as shown in Table 3, the frequency of MRI-visible CSO-PVS gradually decreased as the grade of deep WMH increased (Grade 0, 93.5%; Grade 1, 89.5%; Grade 2–3, 71.0%). The multivariate OR of severe deep WMH for MRI-visible CSO-PVS was 0.68 (95% CI: 0.54–0.86, $P < 0.001$), compared with none or mild deep WMH. Although the age-adjusted OR of severe periventricular WMH for MRI-visible CSO-PVS was 0.85 (0.73–0.98, $P = 0.029$) compared with that of none or mild periventricular WMH, there was not a significant relationship after adjusting for multivariate arteriosclerosis risk factors. The multivariate ORs of deep or periventricular WMH for MRI-visible BG-PVS were approximately 1.2–1.3 and were statistically significant.

Lobar cerebral microbleeds were found in 9 individuals, and deep cerebral microbleeds were found in 13 individuals. Compared to the

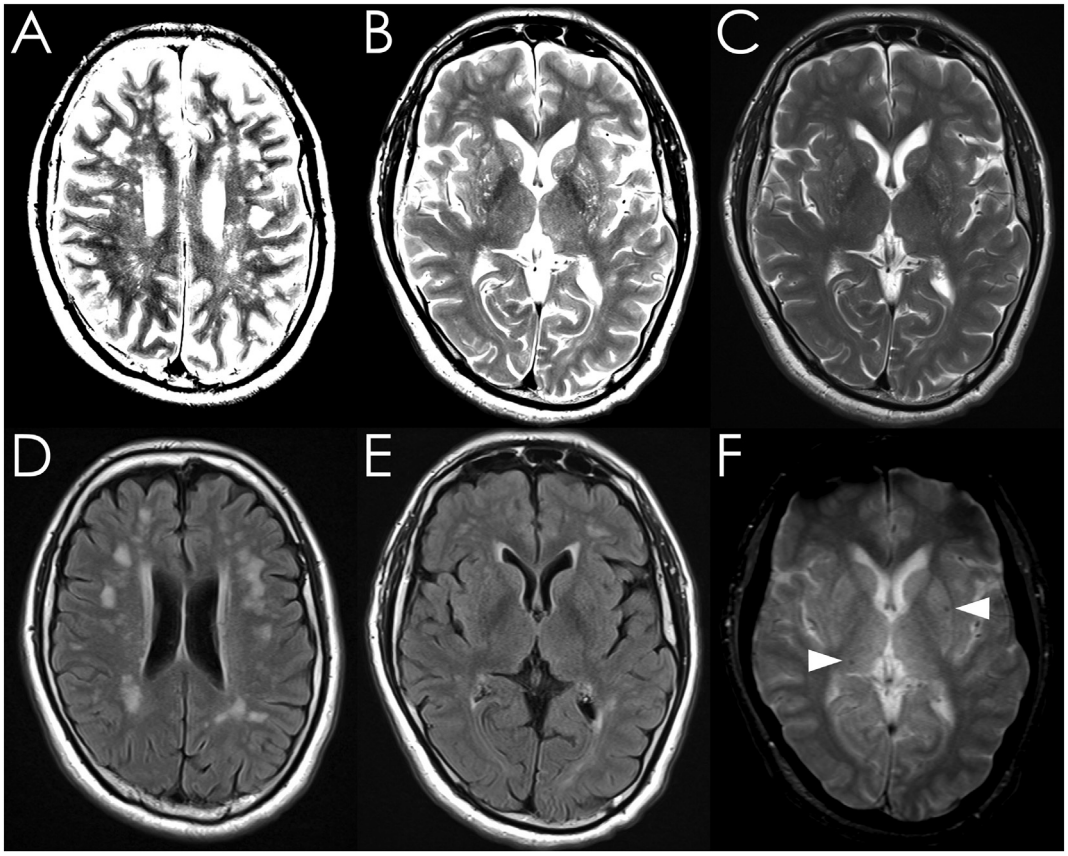

Fig. 1. Perivascular space, white matter hyperintensity and cerebral microbleed. A 61-years healthy man underwent a 3-tesla brain MRI. He was assessed as Grade 1 of perivascular space in the centrum semiovale (CSO-PVS, A) and Grade 2 perivascular space in the basal ganglia (BG-PVS, B), after changing the window level and width from the original T2-weighted images (C). The severity of deep white matter hyperintensity (WMH) was evaluated as Grade 2 (D) and that of periventricular WMH was evaluated as Grade 2 (E) on the FLAIR images. Two deep cerebral microbleeds (white arrowhead) were detected on the T2*-weighted gradient-recalled echo image (F).

274 individuals without cerebral microbleeds, the 13 individuals with deep cerebral microbleeds had a significantly higher prevalence of visible BG-PVS and severe periventricular and deep WMHs (Table 4). There was no significant association between the prevalence of cerebral microbleeds and the grade of CSO-PVS.

In males, the inverse relationship between CSO-PVS and deep WML became stronger (Tables 5 and 6). The multivariate OR of abundant MRI-visible CSO-PVS for the presence of deep WMH in males were 0.83 (0.71–0.97, $P = 0.021$), and that of severe deep WMH for MRI-visible CSO-PVS was 0.60 (0.45–0.81, $P < 0.001$). However, there was no significant relationship in females.

4. Discussion

In the present study, more than 90% of healthy individuals aged 60 years or older without deep WMH on MRI had a considerable number of MRI-visible CSO-PVS, while elderly individuals with deep WMH had significantly fewer CSO-PVS as shown in Fig. 2. Additionally, we confirmed that MRI-visible BG-PVS were significantly associated with the presence and severity of periventricular and deep WMHs. Unlike BG-

Table 1
Clinical characteristics.

	Deep white matter hyperintensity				Periventricular hyperintensity			
	Grade 0	Grade 1	Grade 2–3	*P*	Grade 0	Grade 1	Grade 2–3	*P*
Total number (n = 296)	108	105	83		175	62	59	
Male (n = 222)	90 (83.3%)	75 (71.4%)	57 (68.7%)	0.035	138 (78.9%)	49 (79.0%)	35 (59.3%)	0.011
Smoker (n = 46)	21 (24.1%)	18 (24.0%)	7 (11.7%)	0.118	33 (24.8%)	9 (19.6%)	4 (9.3%)	0.086
Hypertension (n = 91)	27 (31.0%)	31 (41.3%)	33 (55.0%)	0.015	42 (31.6%)	21 (45.7%)	28 (65.1%)	< 0.001
SBP ≥ 130 mmHg (n = 73)	23 (25.8%)	25 (30.1%)	25 (38.5%)	0.243	35 (25.0%)	20 (39.2%)	18 (39.1%)	0.066
DBP ≥ 85 mmHg (n = 22)	6 (6.7%)	6 (7.2%)	10 (15.4%)	0.171	10 (7.1%)	8 (15.7%)	4 (8.7%)	0.195
Dyslipidemia (n = 63)	22 (25.3%)	22 (29.3%)	19 (31.7%)	0.678	32 (24.1%)	16 (34.8%)	15 (34.9%)	0.219
Diabetes mellitus (n = 32)	16 (18.4%)	11 (14.7%)	5 (8.3%)	0.232	21 (15.8%)	9 (19.6%)	2 (4.7%)	0.096
CHD (n = 21)	6 (6.9%)	8 (10.7%)	7 (11.7%)	0.546	12 (9.0%)	2 (4.3%)	7 (16.3%)	0.187
CKD (n = 120)	57 (67.9%)	34 (50.0%)	29 (52.7%)	0.054	78 (61.9%)	25 (59.5%)	17 (43.6%)	0.128
BMI ≥ 25.0 (n = 68)	24 (27.0%)	22 (26.2%)	22 (33.3%)	0.590	37 (26.2%)	15 (29.4%)	16 (34.0%)	0.573

SBP: systolic blood pressure, DBP: diastolic blood pressure, CHD: chronic heart disease.
CKD: chronic kidney disease, which was considered present if the estimated glomerular filtration rate was < 60 mL/min/1.73 m^2, BMI: body mass index.

Table 2
Risks of perivascular spaces for the presence of white matter hyperintensity.

	Deep white matter hyperintensity							
	absence	presence	A-OR	95% CI	*P*	M-OR	95% CI	*P*
	108	188						
Perivascular space in the centrum semiovale								
Grade 0	7	35		reference			reference	
Grade 1	38	41	0.73	(0.62–0.87)	< .001	0.70	(0.54–0.89)	0.005
Grade 2	63	112	0.86	(0.77–0.96)	0.009	0.87	(0.76–1.00)	0.043
Perivascular space in the basal ganglia								
Grade 0	48	40		reference			reference	
Grade 1	43	88	1.25	(1.09–1.42)	< .001	1.18	(0.99–1.40)	0.065
Grade 2	17	60	1.37	(1.18–1.59)	< .001	1.08	(0.87–1.34)	0.479
	Periventricular hyperintensity							
	absence	presence	A-OR	95% CI	*P*	M-OR	95% CI	*P*
	175	121						
Perivascular space in the centrum semiovale								
Grade 0	20	22		reference			reference	
Grade 1	51	28	0.84	(0.70–1.01)	0.063	1.20	(0.92–1.57)	0.180
Grade 2	104	71	0.91	(0.82–1.02)	0.103	1.05	(0.91–1.21)	0.484
Perivascular space in the basal ganglia								
Grade 0	67	21		reference			reference	
Grade 1	86	45	1.14	(0.98–1.32)	0.085	1.10	(0.90–1.35)	0.338
Grade 2	22	55	1.58	(1.38–1.82)	< .001	1.60	(1.28–1.99)	< .001

A-OR: age-adjusted odds ratio for the presence of white matter hyperintensity.
M-OR: multivariate odds ratio for the presence of white matter hyperintensity.

PVS, CSO-PVS is normally visible in healthy elderly individuals on the conventional T2-weighted sequence both of the 1.5T and 3T MRI. These findings are novel but do not conflict with the current understanding of PVS [8,11,13,15,17–19]. Recent articles reported that only BG-PVS, not CSO-PVS, had a significant association with deep WMH in the individuals with cerebral microbleeds or lacunar infarction [8,11,13,18]. This location-specific discrepancy in the relationship between PVS and WMH leads us to believe that the functions and mechanisms of CSO-PVS quite differ from those of BG-PVS. Our hypothesis is supported by recent reports that the anatomical structures of PVS are different between the basal ganglia and deep white matter around the centrum semiovale [12,22]. Additionally, we previously reported that MRI-visible CSO-PVS did not penetrate the subarachnoid space on the brain surface and was not winding or branching like the BG-PVS [23]. The superficial arteriole passing through the brain surface has a smaller flow volume and lower pulse pressure wave amplitude than the lenticulostriate artery passing through the basal ganglia. Based on the Tsunami wave model [24], the impact of arterial pulsation, which is the

Table 3
Risks of white matter hyperintensity for the presence of a visible perivascular space.

	Perivascular space in the centrum semiovale							
	invisible[#]	visible"	A-OR	95% CI	*P*	M-OR	95% CI	*P*
	42	254						
Deep white matter hyperintensity								
Grade 0	7	101		reference			reference	
Grade 1	11	94	0.86	(0.68–1.10)	0.224	0.74	(0.54–1.01)	0.055
Grade 2–3	24	59	0.67	(0.56–0.80)	< .001	0.68	(0.54–0.86)	0.001
Periventricular hyperintensity								
Grade 0	20	155		reference			reference	
Grade 1	9	53	0.94	(0.79–1.11)	0.451	1.05	(0.84–1.31)	0.685
Grade 2–3	13	46	0.85	(0.73–0.98)	0.029	0.93	(0.78–1.12)	0.457
	Perivascular space in the basal ganglia							
	invisible[#]	visible"	A-OR	95% CI	*P*	M-OR	95% CI	*P*
	88	208						
Deep white matter hyperintensity								
Grade 0	48	60		reference			reference	
Grade 1	22	83	1.29	(1.12–1.49)	< .001	1.35	(1.14–1.60)	< .001
Grade 2–3	18	65	1.26	(1.09–1.44)	0.002	1.18	(1.01–1.38)	0.036
Periventricular hyperintensity								
Grade 0	67	108		reference			reference	
Grade 1	13	49	1.16	(1.03–1.30)	0.014	1.21	(1.06–1.38)	0.006
Grade 2–3	8	51	1.21	(1.08–1.35)	< .001	1.17	(1.03–1.33)	0.015

A-OR: age-adjusted odds ratio for the presence of white matter hyperintensity.
M-OR: multivariate odds ratio for the presence of white matter hyperintensity.
invisible[#]: perivascular space Grade 0.
visible": perivascular space Grade 1–2.

Table 4
Prevalence of white matter hyperintensity (WMH) and MRI-visible perivascular spaces (PVS) with or without a cerebral microbleed (CMB).

	Lobar CMB	Deep CMB	Non-CMB	*P*1	*P*2	*P*3
	9	13	274			
Perivascular space in the centrum semiovale				0.166	0.446	0.258
Grade 0	1 (11.1%)	3 (23.1%)	38 (13.9%)			
Grade 1	4 (44.4%)	1 (7.7%)	74 (27.0%)			
Grade 2	4 (44.4%)	9 (69.2%)	162 (59.1%)			
Perivascular space in the basal ganglia				0.097	0.627	0.014
Grade 0	4 (44.4%)	1 (7.7%)	83 (30.3%)			
Grade 1	3 (33.3%)	4 (30.8%)	124 (45.3%)			
Grade 2	2 (22.2%)	8 (61.5%)	67 (24.5%)			
Deep white matter hyperintensity				0.076	0.312	0.004
Grade 0	7 (77.7%)	1 (7.7%)	167 (60.9%)			
Grade 1	0	5 (38.5%)	57 (20.8%)			
Grade 2–3	2 (22.2%)	7 (53.8%)	50 (18.2%)			
Periventricular hyperintensity				0.003	0.350	< .001
Grade 0	5 (55.5%)	1 (7.7%)	102 (37.2%)			
Grade 1	1 (11.1%)	3 (23.1%)	101 (36.9%)			
Grade 2–3	3 (33.3%)	9 (69.2%)	71 (25.9%)			

*P*1; probability value of lobar CMB vs. deep CMB.
*P*2; probability value of lobar CMB vs. non-CMB.
*P*3; probability value of deep CMB vs. non-CMB.

main driving force of the bulk flow of cerebrospinal fluid in the PVS [25,26], might be larger in the basal ganglia (i.e., BG-PVS) rather than that in the centrum semiovale (i.e., CSO-PVS). Therefore, BG-PVS was proposed as an imaging biomarker related with hypertensive arteriopathy or arteriosclerosis [18], whereas CSO-PVS was related with cerebral amyloid angiopathy, which is associated with amyloid-β deposition at the cerebral capillaries [6–9,13,14,20]. However, there was no significant relationship between CSO-PVS and lobar cerebral microbleeds in this study, because of the low prevalence of cerebral microbleeds. Therefore, we have to build another hypothesis about the inverse relationship between and CSO-PVS and deep WMH. A possible lymphatic drainage of cerebral interstitial fluid to cerebrospinal fluid via PVS has been studied for > 100 years ago by Cushing and Cserr, el al [27,28]. According to the latest concept of the glymphatic pathway, cerebrospinal fluid from the subarachnoid space is driven into the brain parenchyma through the PVS of penetrating arteries on the brain surface, and interstitial fluid in the white matter is drained towards the ventricles through the white matter tracts or PVS of deep cerebral veins [3]. Mechanisms are still far from understood, but PVS in the white matter might work as a glymphatic efflux via the space between the white matter fibers or venous PVS rather than glymphatic influx via the arterial PVS. On the other hand, recent accumulated evidence suggests that deep WMH has several etiologies, such as arterial endothelial damage, demyelination, glial scarring, ischemia, inflammation and permeability change with leakage of solute in the blood-brain barrier [12,16]. Therefore, deep WMH related to dysfunction of the astrocyte barrier might induce the disruption of perivascular structures such as the endothelial basement membrane, pericytes, leptomeninges, parenchymal basement membrane and astrocyte endfeet [29].

Our study has several limitations. First, we were unable to determine a causal relationship between CSO-PVS and deep WMH because this study used a cross-sectional design. The progression of deep

Table 5
Risks of perivascular spaces for the presence of white matter hyperintensity in males.

	Deep white matter hyperintensity							
	Absence	Presence	A-OR	95%CIs	*P* value	M-OR	95%CIs	*P* value
	90	132						
Perivascular space in centrum semiovale								
Grade 0	5	27		reference			reference	
Grade 1	35	27	0.69	(0.57–0.83)	< 0.001	0.63	(0.48–0.82)	< 0.001
Grade 2	50	78	0.84	(0.73–0.95)	0.007	0.83	(0.71–0.97)	0.021
Perivascular space in basal ganglia								
Grade 0	43	29		reference			reference	
Grade 1	32	64	1.31	(1.13–1.52)	< 0.001	1.21	(0.99–1.48)	0.067
Grade 2	15	39	1.36	(1.15–1.61)	< 0.001	1.12	(0.89–1.41)	0.332
	Periventricular hyperintensity							
	absence	presence	A-OR	95%CIs	*P* value	M-OR	95%CIs	*P* value
	138	84						
Perivascular space in centrum semiovale								
Grade 0	15	17		reference			reference	
Grade 1	44	18	0.79	(0.65–0.97)	0.023	1.21	(0.87–1.68)	0.255
Grade 2	79	49	0.90	(0.79–1.02)	0.090	1.05	(0.90–1.23)	0.527
Perivascular space in basal ganglia								
Grade 0	57	15		reference			reference	
Grade 1	65	31	1.16	(0.98–1.38)	0.084	1.14	(0.90–1.46)	0.279
Grade 2	16	38	1.64	(1.40–1.92)	< 0.001	1.62	(1.25–2.10)	< 0.001

A-OR: age-adjusted odds ratio for the presence of white matter hyperintensity.
M-OR: multivariate odds ratio for the presence of white matter hyperintensity.

Table 6
Risks of white matter hyperintensity for the presence of a visible perivascular space in males.

	Perivascular space in centrum semiovale							
	invisible[#]	visible"	A-OR	95%CIs	*P* value	M-OR	95%CIs	*P* value
	32	190						
Deep white matter hyperintensity								
Grade 0	5	85		reference			reference	
Grade 1	9	66	0.81	(0.61–1.06)	0.120	0.64	(0.45–0.92)	0.015
Grade 2–3	18	39	0.63	(0.51–0.77)	< 0.001	0.60	(0.45–0.81)	< 0.001
Periventricular hyperintensity								
Grade 0	15	123		reference			reference	
Grade 1	8	41	0.90	(0.75–1.09)	0.293	0.99	(0.77–1.27)	0.923
Grade 2–3	9	26	0.81	(0.69–0.96)	0.016	0.95	(0.77–1.18)	0.649
	Perivascular space in basal ganglia							
	invisible[#]	visible"	A-OR	95%CIs	*P* value	M-OR	95%CIs	*P* value
	72	150						
Deep white matter hyperintensity								
Grade 0	43	47		reference			reference	
Grade 1	17	58	1.30	(1.12–1.52)	< 0.001	1.34	(1.11–1.61)	0.002
Grade 2–3	12	45	1.31	(1.12–1.53)	< 0.001	1.22	(1.03–1.44)	0.019
Periventricular hyperintensity								
Grade 0	57	81		reference			reference	
Grade 1	9	40	1.21	(1.06–1.37)	0.004	1.23	(1.07–1.43)	0.005
Grade 2–3	6	29	1.17	(1.04–1.32)	0.009	1.13	(0.99–1.29)	0.066

A-OR: age-adjusted odds ratio for the presence of white matter hyperintensity.
M-OR: multivariate odds ratio for the presence of white matter hyperintensity.
invisible[#]: perivascular space Grade 0.
visible": perivascular space Grade 1–2.

WMH in CSO-PVS should be examined in a longitudinal cohort study. Second, the prevalence of cerebral microbleeds in our healthy elderly participants without cerebrovascular disease was 7.4%, which was too low for statistical analysis. However, the prevalence of cerebral microbleeds in elderly subjects without cerebrovascular disease was reported to be between 5% and 6% [30]. Third, we evaluated the severity of PVS and WMH using visual scales and not quantitative volumetric techniques. However, a quantitative method for counting PVS has not been established, and visual semi-quantitative assessment is still the standard method. Fourth, we mentioned about sex differences in the association between PVS and WMH, regardless of unidentified mechanisms. Because only 25% of the participants were female, we considered that the sample size of female might be too small for statistical analysis. Finally, the influence of magnetic field strength of MRI could not be ignored. Indeed, the frequency of invisible CSO-PVS on 3T MRI was 6.5%, which was significantly lower than that on 1.5T MRI (19.8%) in this study. Therefore, we investigated the association between PVS and WMH after stratification by the magnetic field strength, but there was no particular trend observed.

5. Conclusions

Different mechanisms may account for PVS according to their anatomical distribution. BG-PVS was significantly increased in elderly individuals with deep and periventricular WMHs. Conversely, CSO-PVS was significantly decreased in elderly individuals with deep WMH. The inverse relationship between CSO-PVS and deep WMH may provide valuable information for future studies of mechanisms of the glymphatic pathway. Specifically, PVS in the white matter might play an essential role as the brain's interstitial fluid drainage system, not as the biomarkers of arteriosclerosis and cerebral amyloid angiopathy.

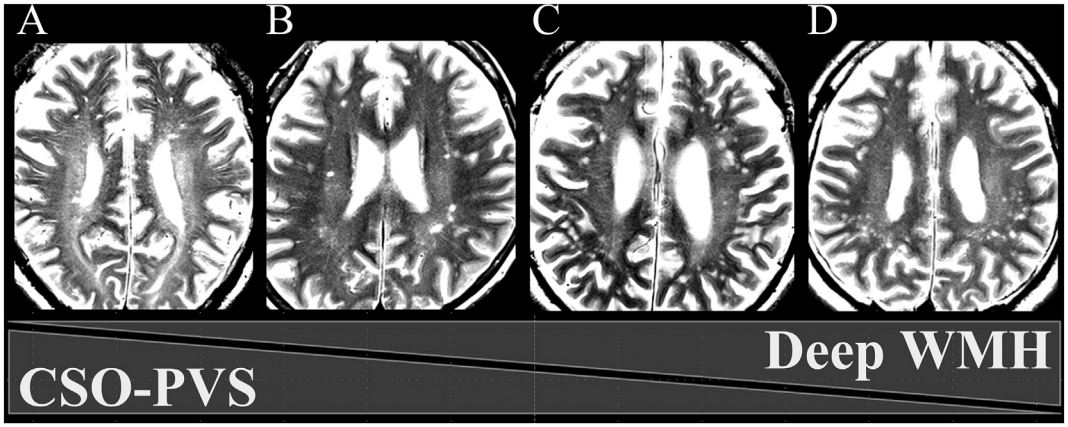

Fig. 2. Perivascular space and white matter hyperintensity on T2-weighted image. These images show the representative cases for an inverse relationship between PVS in the centrum semiovale (CSO-PVS) and deep WMH. There were more abundant visible CSO-PVS on the left side. Grades of the CSO-PVS and deep WMHs were 2 and 0 in A, 1 and 1 in B, 1 and 2 in C, and 0 and 2 in D, respectively.

Acknowledgements

We would like to thank the staff at the Department of Radiology in our institute.

References

[1] J.J. Iliff, M. Wang, Y. Liao, B.A. Plogg, W. Peng, G.A. Gundersen, et al., A paravascular pathway facilitates CSF flow through the brain parenchyma and the clearance of interstitial solutes, including amyloid beta, Sci. Transl. Med. 4 (2012) 147ra11.
[2] M. Nedergaard, Neuroscience. Garbage truck of the brain, Science 340 (2013) 1529–1530.
[3] M.K. Rasmussen, H. Mestre, M. Nedergaard, The glymphatic pathway in neurological disorders, The Lancet Neurology. 17 (2018) 1016–1024.
[4] J.J. Iliff, M. Nedergaard, The Glymphatic System and Brain Interstitial Fluid Homeostasis. Primer on Cerebrovascular Diseases, Second Edition, (2017), pp. 17–25 Elsevier Inc.
[5] D.M. Zeppenfeld, M. Simon, J.D. Haswell, D. D'Abreo, C. Murchison, J.F. Quinn, et al., Association of perivascular localization of aquaporin-4 with cognition and alzheimer disease in aging brains, JAMA neurology. 74 (2017) 91–99.
[6] A. Charidimou, R. Meegahage, Z. Fox, A. Peeters, Y. Vandermeeren, P. Laloux, et al., Enlarged perivascular spaces as a marker of underlying arteriopathy in intracerebral haemorrhage: a multicentre MRI cohort study, J. Neurol. Neurosurg. Psychiatry 84 (2013) 624–629.
[7] A. Charidimou, R.H. Jager, A. Peeters, Y. Vandermeeren, P. Laloux, J.C. Baron, et al., White matter perivascular spaces are related to cortical superficial siderosis in cerebral amyloid angiopathy, Stroke 45 (2014) 2930–2935.
[8] A. Charidimou, G. Boulouis, M. Pasi, E. Auriel, E.S. van Etten, K. Haley, et al., MRI-visible perivascular spaces in cerebral amyloid angiopathy and hypertensive arteriopathy, Neurology 21 (2017) 1157–1164.
[9] A. Charidimou, G. Boulouis, M.E. Gurol, C. Ayata, B.J. Bacskai, M.P. Frosch, et al., Emerging concepts in sporadic cerebral amyloid angiopathy, Brain J. Neurol. 140 (2017) 1829–1850.
[10] L.A. Heier, C.J. Bauer, L. Schwartz, R.D. Zimmerman, S. Morgello, M.D. Deck, Large Virchow-Robin spaces: MR-clinical correlation, AJNR Am. J. Neuroradiol. 10 (1989) 929–936.
[11] C.M. Loos, P. Klarenbeek, R.J. van Oostenbrugge, J. Staals, Association between perivascular spaces and progression of white matter hyperintensities in lacunar stroke patients, PLoS One 10 (2015) e0137323.
[12] J.M. Wardlaw, E.E. Smith, G.J. Biessels, C. Cordonnier, F. Fazekas, R. Frayne, et al., Neuroimaging standards for research into small vessel disease and its contribution to ageing and neurodegeneration, The Lancet Neurology. 12 (2013) 822–838.
[13] Y. Yakushiji, A. Charidimou, M. Hara, T. Noguchi, M. Nishihara, M. Eriguchi, et al., Topography and associations of perivascular spaces in healthy adults: the Kashima scan study, Neurology 83 (2014) 2116–2123.
[14] S. Yang, W. Qin, L. Yang, H. Fan, Y. Li, J. Yin, et al., The relationship between ambulatory blood pressure variability and enlarged perivascular spaces: a cross-sectional study, BMJ Open 7 (2017) e015719.
[15] J. Ding, S. Sigurethsson, P.V. Jonsson, G. Eiriksdottir, A. Charidimou, O.L. Lopez, et al., Large perivascular spaces visible on magnetic resonance imaging, cerebral small vessel disease progression, and risk of dementia: the age, gene/environment susceptibility-reykjavik study, JAMA Neurol. 74 (2017) 1105–1112.
[16] E.A. Nagelhus, O.P. Ottersen, Physiological roles of aquaporin-4 in brain, Physiol. Rev. 93 (2013) 1543–1562.
[17] R. Hurford, A. Charidimou, Z. Fox, L. Cipolotti, R. Jager, D.J. Werring, MRI-visible perivascular spaces: relationship to cognition and small vessel disease MRI markers in ischaemic stroke and TIA, J. Neurol. Neurosurg. Psychiatry 85 (2014) 522–525.
[18] I. Riba-Llena, J. Jimenez-Balado, X. Castane, A. Girona, A. Lopez-Rueda, X. Mundet, et al., Arterial stiffness is associated with basal ganglia enlarged perivascular spaces and cerebral small vessel disease load, Stroke 49 (2018) 1279–1281.
[19] Y.C. Zhu, C. Tzourio, A. Soumare, B. Mazoyer, C. Dufouil, H. Chabriat, Severity of dilated Virchow-Robin spaces is associated with age, blood pressure, and MRI markers of small vessel disease: a population-based study, Stroke 41 (2010) 2483–2490.
[20] M. Ishikawa, S. Yamada, K. Yamamoto, Dilated perivascular spaces in the centrum semiovale begin to develop in middle age, J. Alzheimers Dis.: JAD. 61 (2018) 1619–1626.
[21] F. Fazekas, J.B. Chawluk, A. Alavi, H.I. Hurtig, R.A. Zimmerman, MR signal abnormalities at 1.5 T in Alzheimer's dementia and normal aging, AJR Am. J. Roentgenol. 149 (1987) 351–356.
[22] E.T. Zhang, C.B. Inman, R.O. Weller, Interrelationships of the pia mater and the perivascular (Virchow-Robin) spaces in the human cerebrum, J. Anat. 170 (1990) 111–123.
[23] M. Ishikawa, S. Yamada, K. Yamamoto, Three-dimensional observation of Virchow-Robin spaces in the basal ganglia and white matter and their relevance to idiopathic normal pressure hydrocephalus, Fluids and barriers of the CNS. 12 (2015) 15.
[24] N. Saji, K. Toba, T. Sakurai, Cerebral small vessel disease and arterial stiffness: tsunami effect in the brain? Pulse (Basel). 3 (2016) 182–189.
[25] J.J. Iliff, M. Wang, D.M. Zeppenfeld, A. Venkataraman, B.A. Plog, Y. Liao, et al., Cerebral arterial pulsation drives paravascular CSF-interstitial fluid exchange in the murine brain, J. Neurosci. 33 (2013) 18190–18199.
[26] M.A. Stoodley, S.A. Brown, C.J. Brown, N.R. Jones, Arterial pulsation-dependent perivascular cerebrospinal fluid flow into the central canal in the sheep spinal cord, J. Neurosurg. 86 (1997) 686–693.
[27] H.F. Cserr, Relationship between cerebrospinal fluid and interstitial fluid of brain, Fed. Proc. 33 (1974) 2075–2078.
[28] H. Cushing, Studies on the cerebro-spinal fluid: I. Introduction, J. Med. Res. 31 (1914) 1–19.
[29] M.V. Sofroniew, Astrocyte barriers to neurotoxic inflammation, Nat. Rev. Neurosci. 16 (2015) 249–263.
[30] H.C. Koennecke, Cerebral microbleeds on MRI: prevalence, associations, and potential clinical implications, Neurology 66 (2006) 165–171.